



Computer study of the removal of Cu from the graphene surface using Ar clusters



Alexander Y. Galashev

Institute of Industrial Ecology, Ural Branch of the Russian Academy of Sciences, Sofia Kovalevskaya Str. 20, Ekaterinburg 620990, Russia

ARTICLE INFO

Article history:

Received 6 August 2014
Received in revised form 29 October 2014
Accepted 3 November 2014
Available online xxxx

Keywords:

Argon cluster bombardment
Copper film
Graphene

ABSTRACT

The method of molecular dynamics has been used to study the bombardment of a copper film on supported graphene by Ar₁₃ clusters with kinetic energies of 5, 10, 20 and 30 eV and different angles of incidence. It is obtained that the cluster energy should be in the interval 20–30 eV for effective graphene cleaning. There is no cleaning effect at vertical incidence ($\theta = 0^\circ$) of Ar₁₃ clusters. The bombardments at 45° and 90° incident angles are the most effective ones at a moderate and big amount of deposited copper respectively.

© 2014 Elsevier B.V. All rights reserved.

1. Introduction

Graphene has unique physical properties and energy-band structure. It is possible now to receive graphene of a small size with the help of different technologies. However, there is a new technology of graphene film production of the size up to 70 cm [1]. Graphene can be used in different membranes due to its highest flexibility and mechanical strength. As an absorbing material, graphene is an effective one only in the case of multiple using. Consequently the question of graphene cleaning of deposited substances arises. In addition there was a need to develop an effective method for releasing copper from scrap copper-graphene electrodes recently used in electrochemical devices operating in aggressive environments. Graphene coating on copper significantly (by one and half orders of magnitude) increases the resistance of the metal to electrochemical degradation. The copper has a significant practical interest. The surface pollutions on graphene are removed by ion beam [2]. The bombardment with the cluster beam can be effective method of graphene cleaning. It is important here however to find the correct bombardment energy to avoid the damage of graphene membrane. Molecular dynamics (MD) simulation of plasma interaction on a graphite surface has shown that the graphite surface absorbs the most part of hydrogen atoms when the energy of incident beam is 5 eV [3]. At the same time almost all hydrogen atoms are reflected from the surface at the beam energy 15 eV. Vertical bombardment by Ar₁₀ clusters with kinetic energy $E_k < 30$ eV executed in MD model does not result in the

break of graphene sheet during 100 runs [4]. Graphene is broken at $E_k = 40$ eV.

The ion track lithographic method uses the passage of energetic ions through nanoholes in the mask and subsequent bombing of the graphene sheet only within a limited nanoregion. It is important to investigate in detail the entire lithographic process to predict how nanostructures can be produced in the suspended graphene sheet using this method. The present study will contribute to achieving this goal. Controlled ion parameters obtained in our simulation will be used to obtain desirable defective structures. No experimental studies have been performed so far to produce such cluster ions to irradiate the target containing graphene. Furthermore, it has been shown that the theory of irradiation effects for bulk targets does not always lead to satisfactory results for the low-dimensional materials, such as graphene [5,6]. It is quite obvious that atomically thin target of graphene requires explicit consideration of the atomic structure [7,8].

The aim of the present work is to investigate stability of the thin copper film on graphene under Ar₁₃ clusters bombardment with kinetic energies 5, 10, 20 and 30 eV and incident angles of the cluster beam 90°, 75°, 60°, 45° and 0°.

2. Material and methods

Interatomic interactions in graphene were described in terms of the modified Tersoff many-body potential [9,10]. Atomic interactions in the copper film were modeled with the use of the Sutton-Chen many-body potential [11]. The copper-carbon interaction was described by the Morse potential [12]. In the Ar₁₃ cluster, the

E-mail address: alexander-galashev@yandex.ru

atoms were supposed to interact via the Lennard–Jones potential [13]. The interaction between Ar atoms and the target (Cu and C) atoms was defined by the purely repulsive Molier potential [14]. We neglect weak attraction between the Ar and Cu atoms on the one hand and the Ar and C atoms on the other hand, since the primary subject of this study is energy and momentum transfer not chemical bonding.

Graphene sheet is placed on a copper substrate which does not allow C atoms to move vertically downwards. Thereby the movement of the sheet under the influence of cluster impacts was completely excluded. Copper substrate was a slice of five atomic layers of the FCC lattice, the lattice (100) plane served as a surface of the slice. This surface has a square shape, 10 atoms Cu are located along the edge of this square, and the entire slice contained 1000 Cu atoms. Graphene sheet of size 3.4×2.8 nm containing 406 atoms of C is placed on the substrate and fully fitted into this square. In the chosen coordinate system the graphene sheet had “zigzag” edges along the x axis and the “armchair” edges – in the direction of the y axis. Initially all the atoms C have coordinates $z = 0$. Substrate atoms were fixed, but interacted with C atoms of the graphene and Cu atoms of the film. Boundary conditions at the edges of graphene were free. It allows investigating the stability of edges to external dynamic loads.

The copper film formation on the graphene was simulated by separate MD calculation in two steps. At the first step Cu atoms were placed over the centers of noncontiguous graphene cells so that the distance between Cu and C atoms would be equal to the distance of 2.243 Å calculated by the density functional theory [15]. Onto this loose film consisting of 49 copper atoms, another 51 Cu atoms were deposited at random. In the initial state copper film presented three-dimensional structure with an ordered lower base (adjacent to graphene) and irregular and not flat top layer. Then the system composed of 100 Cu atoms and 406 C atoms was equilibrated in the MD calculation over a duration of 1 million time steps ($\Delta t = 0.2$ fs). Numerical solution of the equations of motion was carried out by the fourth-order Runge–Kutta method. The target obtained in this manner was subsequently bombarded with icosahedral Ar_{13} clusters during 1 ns.

In the case of vertical bombardment ($\theta = 0^\circ$) the virtual rectangular two-dimensional 5×5 grid covers the graphene sheet. Virtual grid is lifted over graphene sheet at a distance of 1.5 nm. Every grid node gives the initial position for Ar_{13} cluster living 8 ps. The lifetime includes time of flight and time of interaction with the target. After this time Ar atoms of decayed cluster were excluded from consideration and a new cluster Ar_{13} was launched from a different point cluster sources. In the case of inclined bombardment five starting points for placing the centers of the Ar_{13} clusters were uniformly spaced apart on a line parallel to the oy axis (chair direction). This line was displaced to the left (along the ox axis) from the left edge of graphene by a distance of 1.5 nm and raised to such a height (in the direction of the oz axis) to provide an effective impact to the copper film. Interval equal to the L_x length of the graphene sheet in the axial direction (the direction of zigzag) was divided into 5 equal segments of length $L_i = L_x/25$. Five point cluster sources moved horizontally forward at a distance L_i at the beginning of each cycle (except for the first), thus the cluster impacts line moved. As a result, graphene sheet was covered with 125 evenly spaced points to target cluster impacts.

Because of system geometry, it is necessary to investigate separately the horizontal D_{xy} and vertical D_z components of self-diffusion coefficient. Stresses calculation in metal film is described in [11]. Stresses distribution in graphene is obtained by calculating of ratio of the corresponding resultant force acting on a selected site to the area of this site. The surface roughness is calculated as an average arithmetic deviation of surface profile.

3. Calculation

The calculations were performed by the classical molecular dynamics method. In this study, we used three types of empirical potentials describing the carbon–carbon (in graphene), copper–copper, and copper–carbon interactions. The representations of the interactions in graphene were based on the use of the Tersoff potential [9]

$$V_{ij} = f_C(r_{ij})[A \exp(-\lambda^{(1)} r_{ij}) - B b_{ij} \exp(-\lambda^{(2)} r_{ij})], \quad (1)$$

$$f_C(r_{ij}) = \begin{cases} 1, & r_{ij} < R^{(1)} \\ \frac{1}{2} + \frac{1}{2} \cos[\pi(r_{ij} - R^{(1)})/(R^{(2)} - R^{(1)})], & R^{(1)} < r_{ij} < R^{(2)}, \\ 0 & r_{ij} > R^{(2)} \end{cases}, \quad (2)$$

where b_{ij} is the multi-particle bond-order parameter describing in what manner the bond-formation energy (attractive part V_{ij}) is created at local atomic arrangement because of the presence of neighboring atoms. The potential energy is a multi-particle function of atomic positions i, j, k and is determined by parameters

$$b_{ij} = (1 + \beta^n \xi_{ij}^{n_i})^{-1/(2n)}, \quad (3)$$

$$\xi_{ij} = \sum_{k \neq i, j} f_C(r_{ik}) g(\theta_{ijk}), \quad (4)$$

$$g(\theta_{ijk}) = 1 + \frac{c^2}{d^2} - \frac{c^2}{[d^2 + (h - \cos \theta_{ijk})^2]}, \quad (5)$$

where ξ is the effective coordination number, $g(\theta_{ijk})$ is a function of the angle between r_{ij} and r_{ik} which stabilizes the tetrahedral structure.

This potential was successfully tested on many single- and multi-component systems with covalent chemical bonding [16,17]. However, the transition to the simulation of two-dimensional systems (for example, in graphene) with covalent bonding revealed some difficulties in using this potential. The main disadvantages were as follows: the interaction was represented only by short-range covalent forces, and the contributions from the interactions with neighbors of the second and higher orders were not considered. The simulation with this potential led to cracking the graphene sheet even at low temperatures. Another serious disadvantage was in the existence of the net torsional moment appearing because of the lack of mutual compensation of the torsional moments determined by bonds around each atom. As a result, there occurred rotation of the graphene sheet (most frequently, counterclockwise). This effect impeded simulation of nanocomposites and made difficult structural analysis. In the proposed model, the aforementioned disadvantages were eliminated as follows. The scale of covalent interaction in the model was increased from 0.21 to 0.23 nm. Outside the covalent interaction, we used a very weak attractive Lennard–Jones interaction with the parameters taken from [10]. To prevent rotation of the graphene sheet, the “retardation” at each atomic site of the graphene atomic was provided by the force $-dV_{ij}(\Omega_{kijl})/dr_{ij}$ where the torsional potential $V_{ij}(\Omega_{kijl})$ is represented by the expression [10]

$$V_{ij}^{tors}(\Omega_{kijl}) = \varepsilon_{kijl} \left[\frac{256}{405} \cos^{10} \left(\frac{\Omega_{kijl}}{2} \right) - \frac{1}{10} \right], \quad (6)$$

and the torsion angle Ω_{kijl} is defined as the angle between the planes, of which one plane is specified by the vectors \mathbf{r}_{ik} and \mathbf{r}_{ij} , and the other plane, by the vectors \mathbf{r}_{ij} and \mathbf{r}_{jl} :

$$\cos \Omega_{kijl} = \frac{\mathbf{r}_{ji} \times \mathbf{r}_{ik} \cdot \mathbf{r}_{ij} \times \mathbf{r}_{jl}}{|\mathbf{r}_{ji} \times \mathbf{r}_{ik}| \cdot |\mathbf{r}_{ij} \times \mathbf{r}_{jl}|}. \quad (7)$$

The height of the barrier ε_{kijl} for the rotation was taken from [10].

The Sutton–Chen potential was successfully used for simulating both bulk metals and metallic clusters [18]. The Sutton–Chen potential energy is written as

$$U^{SC} = \varepsilon \left[\frac{1}{2} \sum_i \sum_{j \neq i} V(r_{ij}) - c \sum_i \sqrt{\rho_i} \right], \quad (8)$$

where

$$V(r_{ij}) = (a/r_{ij})^n, \quad \rho_i = \sum_{j \neq i} (a/r_{ij})^m, \quad (9)$$

where ε is a parameter having the dimensionality of energy; c is the dimensionless parameter; a is a parameter having the dimensionality of length that is commonly chosen to be the lattice parameter; and m and n are positive integers ($n > m$). The power form of the contributions makes it possible to successfully joint the short-range interactions which are represented by an N -particle terms with the Van der Waals “tail” that determines long-range interaction. For copper, we used the Sutton–Chen potential parameters as follows: $m = 6$, $n = 9$, $\varepsilon = 12.382$ meV, and $c = 39.432$ [18]. The copper–carbon interaction was described using the Morse potential:

$$V(r_{ij}) = D_0 (\exp[-2\alpha(r_{ij} - r_m)] - 2 \exp[-\alpha(r_{ij} - r_m)]). \quad (10)$$

The simulation was performed with the Morse potential parameters as follows: $D_0 = 87$ meV, $\alpha = 17$ nm⁻¹, and $r_m = 0.22$ nm [12].

The interaction between the Ar atoms and the atoms (Cu and C) of the target was determined by purely repulsive Molire potential [14]

$$\Phi = Z_i Z_j \times \frac{e^2}{r} \left\{ 0.35 \exp\left(-0.3 \frac{r}{a}\right) + 0.55 \exp\left(-1.2 \frac{r}{a}\right) + 0.10 \exp\left(-6.0 \frac{r}{a}\right) \right\}, \quad (11)$$

where Z_i and Z_j are atomic numbers of the i and j atoms, e is the elementary charge, r is the distance between the atoms, a is Firsov screening length [19].

$$a = 0.885 a_0 (Z_i^{1/2} + Z_j^{1/2})^{-2/3}. \quad (12)$$

Here a_0 is the Bohr radius.

The stress at the site of the i th atom of the metallic film is defined as [18]

$$\sigma_{\alpha\beta}(i) = \frac{\varepsilon}{2a^2 \Omega_i} \sum_{j \neq i}^k \left[-n(a/r_{ij})^{n+2} + mc \left(1/\sqrt{\rho_i} + 1/\sqrt{\rho_j} \right) (a/r_{ij})^{m+2} \right] r_{ij}^\alpha r_{ij}^\beta, \quad (13)$$

where the volume corresponding to an individual atom Ω_i can be associated with the volume of the Voronoi polyhedron related to the i th atom.

To calculate the stresses induced in graphene, the graphene sheet was divided into elementary areas. The atomic stresses $\sigma_j^i(l)$ in the l th elementary area for each of directions x , y and z with a current index J are determined by calculating the atomic kinetic energies at this area and projections of forces acting on the l th area from all other atoms

$$\sigma_j^i(l) = \frac{1}{k} \left\langle \sum_i^k \frac{1}{\Omega} (m v_j^i v_j^i) \right\rangle + \frac{1}{S_l} \left\langle \sum_i^k (f_j^i) \right\rangle, \quad (14)$$

where k is the number of atoms at the l th area; Ω is the volume per atom; m is the atomic mass; v_j^i is the J th velocity projection of atom i ; and S_l is the area of the l th area. Angular brackets indicate the averaging over time. In this case, the compressive stresses can have plus and minus signs, according to directions of forces f_j^i . In this regard, microscopic stress $\sigma_j^i(l)$ differs from macroscopic stress $\bar{\sigma}_j < 0$.

Self-diffusion coefficient was determined by the mean square displacement of the atoms $\langle [\Delta \mathbf{r}(t)]^2 \rangle$ as

$$D = D_{xy} + D_z = \lim_{t \rightarrow \infty} \frac{1}{2\Gamma} \langle [\Delta \mathbf{r}(t)]^2 \rangle, \quad (15)$$

where $\Gamma = 3$ is the dimension of space, D_{xy} and D_z are the horizontal and vertical components of the self-diffusion coefficient.

The surface roughness (or the profile deviation arithmetic average) was calculated as

$$R_a = \frac{1}{N} \sum_{i=1}^N |z_i - \bar{z}|, \quad (16)$$

where N is the number of nodes (atoms) on the surface of graphene z_i is atomic level, \bar{z} is the graphene surface level, z_i and \bar{z} are the values determined at the same time.

4. Results

There is no graphene surface cleaning after vertical bombardment at energy 5–20 eV. Bombardment with the 10 and 20 eV energies gives significant damage of graphene edges up to knocking out carbon atoms. Copper film becomes looser and Cu atoms form a column. The graphene sheet is partly cleaned of copper atoms after bombardment with energy 20 eV at incident angle $\theta = 75^\circ$. Graphene is almost cleaned of Cu atoms at angles $\theta = 45^\circ$ and $\theta = 60^\circ$. In every case after finishing of inclined bombardment the graphene sheet is removed in parallel or perpendicular (down) direction in relation to its initial position. It allowed removing copper from graphene totally only after bombardment at 45° . In the case of bombardment by the method of the “nap of the earth” flight (incident angle 0°) a big amount of metal atoms is still on the graphene surface when the emitted cluster energy is 10 eV. But the number of copper atoms is reduced at energy 20 eV (Fig. 1).

At any cluster incident angle the mobility of Cu atoms in horizontal plane exceeds considerably (in order) the mobility of ones in vertical direction. After the first cycles of cluster impacts there are high values of D_{xy} components, especially at the incident angle $\theta = 60^\circ$ (Fig. 2a). It seems reasonable because the copper film has not yet adapted to the bombardment. The more intensive fluctuations and significantly higher D_{xy} values testify continuous fast destruction of copper film during clusters impacts at incident angle 45° . Vertical components D_z of copper film self-diffusion coefficient have mostly the same behavior as $D_{xy}(n)$ function (Fig. 2b).

Stresses in xy plane of copper film at every bombardment have extensive fluctuations which become weaker during the last

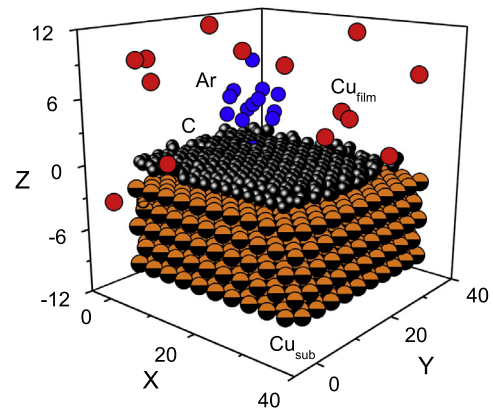


Fig. 1. Configuration of a system “copper film on the graphene sheet with the copper substrate” bombarded by Ar₁₃ cluster with energy 20 eV during final impacts cycle at the incident angle $\theta = 90^\circ$. Coordinates are in angstroms.

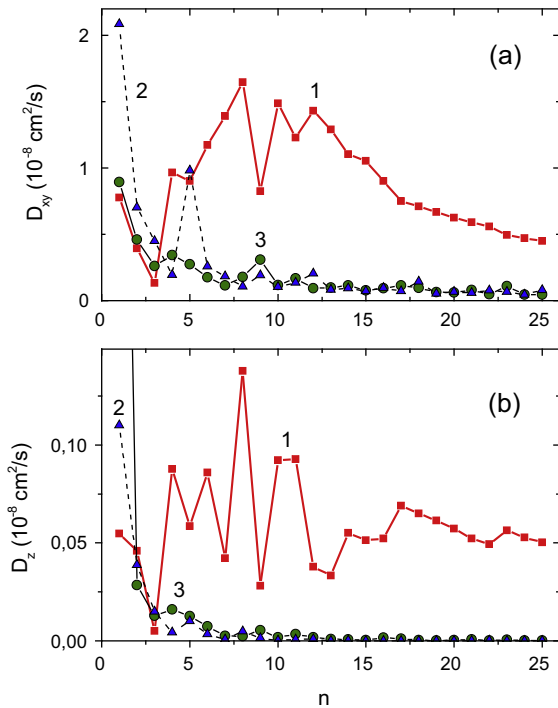


Fig. 2. (a) Horizontal D_{xy} and (b) vertical D_z components of self-diffusion coefficient of Cu film for series of bombardments by Ar_{13} clusters at kinetic energy 20 eV and different incident angles: 1 – 45°, 2 – 60°, 3 – 75°; n is the cycles of 5 impacts each.

impact series. At all incident angles excluding $\theta = 90^\circ$ the σ_{zz} stresses are considerably higher than σ_{zx} and σ_{zy} ones. At $\theta = 90^\circ$ and energy of 10 eV the σ_{zx} , σ_{zy} and σ_{zz} stress components for metal film in horizontal plane have comparably low values during the whole run (Fig. 3a, σ_{zz} is only shown). For the energy 20 eV at the initial target bombardment ($n \leq 10$) there are significant fluctuations of all stress components in horizontal plane. The σ_{zz} component has the most intensive fluctuations. Such fluctuations at energy of bombardment clusters 20 and 30 eV are connected with impacts of Ar atoms compressing the film and knocking out Cu atoms. The fluctuation size of σ_{zz} value is further decreased because of metal film loosening in vertical direction.

On the contrary, stress distribution in the graphene sheet does not almost depend on the direction of incident cluster beam. Cluster impacts are mainly weakened by the copper film. Stresses distribution in graphene between the rows in the “chair” direction at Ar_{13} cluster bombardment with energies 10 and 20 eV at $\theta = 90^\circ$ is shown in Fig. 3b. Because of strong shot-interacting bonds in graphene there are no essential differences between stresses values of σ_{zx} , σ_{zy} and σ_{zz} for series of cluster bombardment with energies 10 and 20 eV. The σ_{zx} and σ_{zy} stresses are uniformly distributed in the plane of graphene sheet. For both energies the maximum σ_{zz} stress in this area of graphene sheet exceeds by 4–7 times the maximum values of σ_{zx} and σ_{zy} stresses. It is connected with impulses transmitted to graphene from Cu atoms which they get as a result of interactions with Ar atoms.

The graphene roughness increases significantly by the end of bombardment. It does not depend on the incident angle and energy of Ar_{13} clusters’ beam. Significant growth of roughness is limited by rigid bonds in graphene. Roughness R_a of the graphene sheet rises nonmonotonically during bombardment (Fig. 4). When the clusters energy is 10 eV the increase of R_a is slow with low amplitudes. There are considerable fluctuations of $R_a(n)$ function especially in the values range of $10 \leq n \leq 25$ when energies are 20 and 30 eV. The decrease of initial growth of roughness in the case of energy 20 eV is connected with the reduction of final R_a value

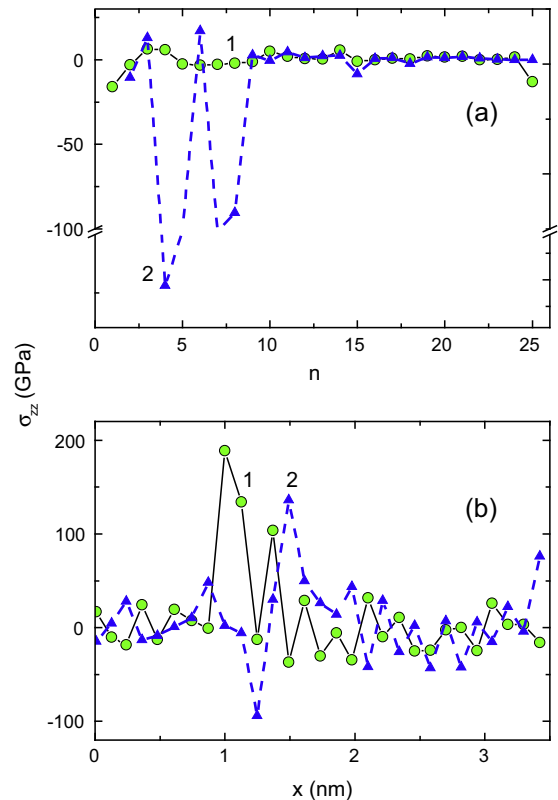


Fig. 3. (a) σ_{zz} stress in xoy plane of metal film and (b) σ_{zz} stresses distribution in the graphene sheet by the rows of C atoms along the “chair” direction for bombardment series by Ar_{13} clusters at incident angle $\theta = 90^\circ$ with energies: 1 – 10 eV, 2 – 20 eV.

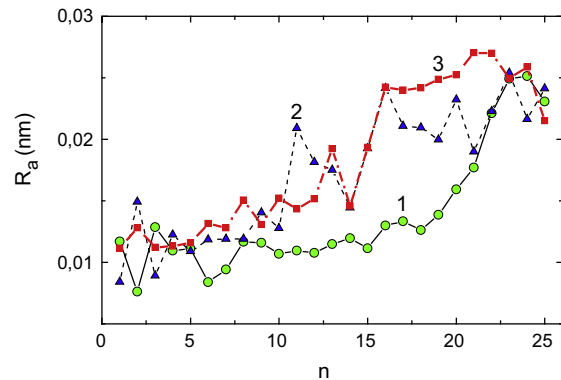


Fig. 4. Roughness of the graphene surface at bombardment of “metal film on the graphene sheet with the copper substrate” system by Ar_{13} clusters at incident angle $\theta = 90^\circ$ with energies: 1 – 10 eV, 2 – 20 eV, 3 – 30 eV.

because of the smoothing effect. At the final bombardment step the Ar_{13} cluster flies rather low over graphene surface and “polishes” it not meeting Cu atoms.

5. Discussion

All graphene-based devices must unavoidably be electrically contacted to outside world by metal contacts. Graphene films can be made by catalytically decomposing hydrocarbon precursors over thin films of copper. Wrinkles in a graphene film have a negative impact on electronic properties by introducing strains that reduce electron mobility. Often the final product must be a single-layer graphene film. Graphene-based membranes could be used to capture carbon dioxide from certain industrial processes, such as coal burning, and thereby reduce greenhouse emissions.

Graphene could cheaply and easily remove salt from seawater. With properly sized holes, graphene sheets may be able to serve as all-purpose filters.

In spray form copper is an ecological threat. Application of graphene oxide as a filter material dramatically increases the efficiency of removal of heavy metals Cu and Pb from an aqueous solution [20]. Removal of trace amounts of heavy metals from water and air is possible through the use of filters with graphene membranes. This however raises the question of filter cleaning from metal deposits. A bond of deposited metal with graphene can be significant because graphene used for membranes has defects such as Stone–Wales defects [21] as well as mono- and poly-vacancies. The method of graphene purification of metal should be on the one hand effective, i.e. able to remove all the sediment, and on the other hand practical enough not to damage graphene and thereby provide its repeated re-use. Argon ion bombardment treatment is effective to remove the oxide film and contamination at the surface [22]. Bombing by a cluster “projectile” is much gentler compared to ion bombardment [23] because cluster “projectile” cannot penetrate the target as deep as the atomic analogue. Under ion bombardment, it is important to choose the angle of incidence of the atomic “projectiles”. For beams of atomic ions the largest ejection of matter is observed at angles of incidence of 40–80° after which the emission starts to decrease [24].

The present study is expected to provide predictive design capability for controlling the surface patterns and stresses in nanotechnology products. For example, the improved understanding could help to make biocompatible surfaces for medical devices. When argon ions hit the copper surface, they penetrate it, knocking away nearby atoms Cu like billiard balls in a process that is akin, at the atomic level, to melting or evaporation.

We carried out the bombardment of graphene by argon clusters with low energy so as not to damage the graphene when cleaning the metal. The cluster bombardment with significantly higher energy can cause sputter of material with covalent bonds as observed when Si is bombarded with 15 keV C_{60}^+ [25]. In this experimental work the incident angle is increased from 0° to 60°. Hill and Blenkinsopp [20] observed a higher sputter yield of Si at 45° than at normal incidence. Molecular dynamics simulations [26] of the bombardment of a silicon crystal with C_{60} are used to understand and interpret the puzzling experimental results [25]. At both incident angles, all of the carbon atoms in the projectile become deposited in the substrate by forming SiC bonds, but for the 45° angle MD simulation more energy is deposited near the surface creating the larger Si yield [26]. Thus, the incident angle of 45° is also the most favorable at sputtering of material with a covalent bond under irradiation of high-energy ion beam.

The stresses in the copper film relax pretty quickly (especially σ_{zz}) as a result of its plasticity and due to a large loss of atoms. Local stresses in graphene relax much more slowly due to the presence of hard bonds and do not disappear even after the bombardment that indicates its crystalline nature. The presence of local stresses even in thermodynamic equilibrium is characteristic feature of ordinary three-dimensional crystals. Instability of two-dimensional crystals with respect to the displacement of atoms in the third dimension is well known and experimentally expressed in a rippled graphene surface [27,28]. This occurs because short-range thermal fluctuations lead to transverse atomic displacements comparable to interatomic distances. Graphene should look like a lattice of cages or a regular stripy pattern with the period equal to 1.8 Å multiplied by an integer [29]. Cluster bombardment of the target greatly enhances this instability and ultimately leads to the surface topography characterized by a large (relative to the value of R_a of non bombarded graphene) roughness.

Graphene sheets on insulating substrates are needed in the traditional electronics. The graphene thin films deposited on

metals are transferred to insulating substrates. However, a new process for the preparation of graphene eliminates this difficult procedure. Argon ion bombardment is widely used in the micro-electronic technology because this noble gas does not react with the carbon. The low temperature (at 300 K) method of fabrication of graphene layers on the top of insulated diamond-like carbon films by moderate energy (~130 eV) ion beam irradiation has been proposed in [30]. Ion beam is capable of inducing the epitaxial crystallization of amorphous layers. The mechanism for such crystallization process involves point defect creation and enhanced diffusion caused by ion bombardment. The process of Cu-film compaction on graphene under the action of Ar_{13} clusters hitting the surface with the energy of 5 eV has been studied in [31]. Graphene exhibited some pliability, and traces of Cu film surface relief remained on it. Classical MD simulations of the bombardment of a graphene sheet by a vertical beam of carbon atoms have been carried out in [32]. The result of the bombardment depends on external conditions, especially, on whether there is a withdrawal of the generated heat. Heat abstraction from the system induces the shift of the beam energy (at which the sample destruction occurs) toward the higher values.

Calculations using density functional theory for the main crystallographic planes of a number of metals, such as Ag, Au, Cu, Pt and Al predict weak binding to graphene [33]. However, there is a group of metals such as Ni, Co, Pd, for which substantially stronger binding is realized due to hybridization between graphene and *d*-metal states. Therefore, the results obtained here for the Cu-coated graphene, are also valid for the cluster bombardment of a graphene sheet with deposited noble metals or aluminum. At the same time it is not critical how the metal is placed on the graphene sheet. However energy of the cluster beam necessary for graphene cleaning may require some adjustment, due to significant differences in masses of the elements.

6. Conclusions

Incident angle $\theta = 45^\circ$ is the most effective one for graphene cleaning of copper by bombardment with argon clusters. Cluster beam energy should be no less than 20 eV. The stresses in the copper film relax rapidly as a result of its plasticity and due to a large loss of atoms. Local stresses in graphene relax much more slowly due to the presence of hard bonds and do not disappear even after the bombardment that indicates its crystalline nature. The presence of local stresses even in thermodynamic equilibrium is characteristic feature of ordinary three-dimensional crystals. Instability of two-dimensional crystals with respect to the displacement of atoms in the third dimension is well known and experimentally expressed in a rippled graphene surface. Cluster bombardment of the target greatly enhances this instability and ultimately leads to the surface topography characterized by a large (relative to the value of R_a of non bombarded graphene) roughness. To use such cleaning method it is important to protect graphene edges because they can be strongly damaged. If it is possible to execute accurate bombardment, the “nap of the earth” flight method is the most effective one here. The total cleaning can be obtained with emitted clusters energy 20 eV and higher. The graphene edges at such cleaning method are less damaged. The prediction model for nanopattern evolution during cluster bombardment can guide the nanomanufacturing processes.

Acknowledgments

This work was supported by the Russian Foundation for Basic Research, Project No. 13-08-00273.

Appendix A. Supplementary material

Supplementary data associated with this article can be found, in the online version, at <http://dx.doi.org/10.1016/j.commatsci.2014.11.002>.

References

- [1] R. Hawaldar, P. Merino, M.R. Correia, I. Bdikin, J. Grácio, J. Méndez, J.A. Martín-Gago, M.K. Singh, *Sci. Rep.* 2 (2012) 682, <http://dx.doi.org/10.1038/srep00682>.
- [2] A. Siokou, F. Ravani, S. Karakalos, O. Frank, M. Kalbac, C. Galiotis, *Appl. Surf. Sci.* 257 (2011) 9785–9790, <http://dx.doi.org/10.1016/j.apsusc.2011.06.017>.
- [3] S. Saito, A. Ito, H. Nakamura, *Plasma Fusion Res.* 5 (2010) S2076, <http://dx.doi.org/10.1585/pfr.5.S2076>.
- [4] N. Inui, K. Mochiji, K. Moritani, *Nanotechnology* 19 (2008) 505501, <http://dx.doi.org/10.1088/0957-4484/19/50/505501>.
- [5] A.V. Krasheninnikov, K. Nordlund, *J. Appl. Phys.* 107 (2010) 071301, <http://dx.doi.org/10.1063/1.3318261>.
- [6] H. Garcia, H. Castán, S. Duenas, L. Bailon, F. Campabadal, J.M. Rafi, I. Tsunoda, *Thin Solid Films* 534 (2013) 482–487, <http://dx.doi.org/10.1016/j.tsf.2013.02.004>.
- [7] A.Y. Galashev, V.A. Polukhin, *Phys. Solid State* 55 (2013) 1733–1738, <http://dx.doi.org/10.1134/S1063783413080118>.
- [8] E. Ahlgren, J. Kotakoski, O. Lehtinen, A.V. Krasheninnikov, *Appl. Phys. Lett.* 100 (2012) 233108, <http://dx.doi.org/10.1063/1.4726053>.
- [9] J. Tersoff, *Phys. Rev. B: Condens. Matter* 37 (1988) 6991–7000, <http://dx.doi.org/10.1103/PhysRevB.37.6991>.
- [10] S.J. Stuart, A.V. Tutein, J.A. Harrison, *J. Chem. Phys.* 112 (2000) 6472–6486, <http://dx.doi.org/10.1063/1.481208>.
- [11] S. Jalili, C. Mochani, M. Akhavan, J. Schofield, *Mol. Phys.* 110 (2012) 267–276, <http://dx.doi.org/10.1080/00268976.2011.640953>.
- [12] A. Oluwajobi, X. Chen, *Int. J. Autom. Comput.* 8 (2011) 326–332, <http://dx.doi.org/10.1007%2Fs11633-011-0588-y>.
- [13] K.-L. Teng, P.-Y. Hsiao, S.-W. Hung, C.-C. Chieng, M.-S. Liu, M.-C. Lu, *J. Nanosci. Nanotechnol.* 8 (2008) 3710, <http://dx.doi.org/10.1166/jnn.2008.007>.
- [14] M.C. Moore, N. Kalyanasundaram, J.B. Freund, H.T. Johnson, *Nucl. Instrum. Method Phys. Res.* 225 (2004) 241–255, <http://dx.doi.org/10.1016/j.nimb.2004.04.175>.
- [15] Z. Xu, M.J. Buehler, *J. Phys.: Condens. Matter* 22 (2010) 485301, <http://dx.doi.org/10.1088/0953-8984/22/48/485301>.
- [16] A.Y. Galashev, *Russ. J. Phys. Chem. B* 6 (2012) 441–447, <http://dx.doi.org/10.1134/S1990793112050041>.
- [17] A.Y. Galashev, *J. Nanopart. Res.* 16 (2013) 2351, <http://dx.doi.org/10.1007/s11051-014-2351-0>.
- [18] H. Rafi-Tabar, *Phys. Rep.* 325 (2000) 239–310, [http://dx.doi.org/10.1016/S0370-1573\(99\)00087-3](http://dx.doi.org/10.1016/S0370-1573(99)00087-3).
- [19] R. Smith, D.E. Harrison Jr., B.J. Garrison, *Phys. Rev. B* 40 (1989) 93–101, <http://dx.doi.org/10.1103/PhysRevB.40.93>.
- [20] Z. Ding, X. Hu, V.L. Morales, B. Gao, *Chem. Eng. J.* 257 (2014) 248–252, <http://dx.doi.org/10.1016/j.cej.2014.07.034>.
- [21] J. Ma, D. Alfè, A. Michaelides, E. Wang, *Phys. Rev. B* 80 (2009) 033407, <http://dx.doi.org/10.1103/PhysRevB.80.033407>.
- [22] A. Wang, O. Ohashi, N. Yamaguchi, M. Aoki, Y. Higashi, N. Hitomi, *Nucl. Instrum. Methods Phys. Res., Sect. B* 206 (2003) 219–223, [http://dx.doi.org/10.1016/S0168-583X\(03\)00732-8](http://dx.doi.org/10.1016/S0168-583X(03)00732-8).
- [23] G. Gillen, S. Roberson, *Rapid Commun. Mass Spectrom.* 12 (1998) 1303–1312, [http://dx.doi.org/10.1002/\(SICI\)1097-0231\(19981015](http://dx.doi.org/10.1002/(SICI)1097-0231(19981015)
- [24] G. Carter, J.S. Colligon, *Ion Bombardment of Solids*, Elsevier Publishing Company Inc., New York, 1968.
- [25] R. Hill, P. Blenkinsopp, *Appl. Surf. Sci.* 231 (2004) 936–939, <http://dx.doi.org/10.1016/j.apsusc.2004.03.177>.
- [26] K.D. Krantzman, D.B. Kingsbury, B.-J. Garrison, *Nucl. Instrum. Methods Phys. Res. B* 255 (2007) 238–241, <http://dx.doi.org/10.1016/j.nimb.2006.11.079>.
- [27] R.E. Peierls, *Ann. Inst. H. Poincaré* 5 (1935) 177–222.
- [28] L.D. Landau, *Phys. Z. Sowjetunion* 11 (1937) 26–35.
- [29] A. O'Hare, F.V. Kusmartsev, K.I. Kugel, *Nano Lett.* 14 (2012) 1–6, dx.doi.org/10.1021/nl204283q.
- [30] S.S. Tinchev, *Appl. Surf. Sci.* 258 (2012) 2931–2934, <http://dx.doi.org/10.1016/j.apsusc.2011.11.009>.
- [31] A.Y. Galashev, V.A. Polukhin, *J. Surf. Invest. X-ray, Synchrotron Neutron Tech.* 8 (2014) 1082–1088.
- [32] O.V. Khomenko, M.V. Prodanov, Yu.V. Scherbak, *J. Nano-Electron. Phys.* 1 (2009) 66–78, doi.org/10.1021/143549d5ee13fe54f5046/1.
- [33] M. Vanin, J.J. Mortensen, A.K. Kelkkanen, J.M. Garcia-Lastra, K.S. Thygesen, K.W. Jacobsen, *Phys. Rev. B* 81 (2010) R081408, <http://dx.doi.org/10.1103/PhysRevB.81.081408>.